# Anesthetic Action on Membrane Lipids†

Tian Yow Tsong,* Martin Greenberg, and Minoru I. Kanehisa

ABSTRACT: The kinetics of the transport of 8-anilino-1-naphthalenesulfonate (ANS) across membrane bilayers have been found to be sensitive to the physical state of the phospholipids (Tsong, *Biochemistry, 14,* 5409 (1975)). We have employed the transport reaction to probe the effect of local anesthetics and sedative hypnotics on synaptosomal and synthetic membranes. In the presence of clinically effective concentrations of local anesthetics, either procaine or lidocaine, the rate of ANS transport in the bilayer dispersions of dimyristoyl-L-α-lecithin increased nearly 100-fold. A 20-fold enhancement was observed in synaptosomal suspensions. In contrast, the sedative hypnotics pentobarbital, γ-butyrolactone, and chloral hydrate showed very little effect on the kinetics of the ANS transport either in the lecithin or synaptosomal suspensions. These findings point to the differing modes of interactions for the local anesthetics and the sedative hypnotics. When ANS transport was measured in the temperature range where the crystalline–liquid crystalline phase transition of the lecithin bilayers occurs, the local anesthetic procaine decreased both the midpoint ($T_m$) and the cooperativity of the phase transition. A cluster model of lipid phase transitions, in which ANS molecules permeate most rapidly through the phase boundaries of the lipid, reproduces semiquantitatively the melting behavior of the lipid–local anesthetics mixtures and the kinetic data. It is concluded that local anesthetics reduce the average size of the lipid clusters. This creates more phase boundaries and permits faster permeation of the dye molecules.

Anesthetics reversibly block a nerve's action potential without appreciably affecting the resting membrane potential (Blaustein, 1968). The sedative hypnotics, a family of anesthetics including barbiturates, block nerve conduction by suppressing the membrane currents of $Na^+$ and $K^+$ ions (Blaustein, 1968; Thesleff, 1956; Naharashi et al., 1969). Another family, the local anesthetics, achieve conduction block by suppressing primarily the initial inrush of sodium current upon neural membrane depolarization (Condouris, 1963). How these anesthetics affect neural membranes and suppress ionic conductances at a molecular level is a question of fundamental importance.

The relatively nonspecific nature of anesthetic action has long been recognized (Seeman, 1975). For example, the potency of an anesthetic appears to depend not on its chemical structure but on its lipid, or more precisely membrane solubility. It was observed that anesthetics cause an expansion of the hydrophobic region of the membrane by about 0.4%, a greater effect than can be accounted for by the volume of anesthetic molecules themselves (Seeman and Roth, 1972). This effect is reversible by the application of external pressure (Miller et al., 1973).

The sites of anesthetic interaction in membranes are obscure. Some investigators have postulated binding to specific membrane proteins (Denburg et al., 1972; Weber and Changeux, 1974; Eyring, 1966). Others believe that the suppression of inward sodium current and outward potassium current depends upon the interaction of anesthetics with specific membrane phospholipids and calcium ions (Papahadjopoulos, 1972; Blaustein and Goldman, 1966). Recent studies of the anesthetic effect on synthetic membranes suggest an increase in fluidity of the bilayers (Trudell et al., 1975; Lee et al., 1974; Jain et al., 1975; Miller and Pang, 1976). This alteration in lipid fluidity may impose conformational changes of membrane proteins specific to sodium or potassium transport (Lee, 1976).

In a recent communication we have reported that the transport of ANS[1] or bromothymol blue into lipid bilayers is sensitive to the physical state of the lipid (Tsong, 1975a,b). We employ this reaction to probe the effect of anesthetics on synaptosomal membranes and DML dispersions. It will be shown that the mode of action of local anesthetics is distinctively different from that of sedative hypnotics on neural membranes and phospholipid bilayers. The experimental results obtained can be reproduced semiquantitatively by a cluster model of lipid phase transitions (Minoru I. Kanehisa and Tian Yow Tsong, manuscript in preparation).

## Materials and Methods

*Synaptosomes.* Synaptosomes were prepared by modifying the method of Hoss and Abood (1974). Ten grams of fresh beef cerebral cortex was homogenized in 100 mL of 0.32 M sucrose with an all-glass Thomas tissue grinder (six up and down strokes), and centrifuged at 1000*g* for 10 min in a Sorvall RC2-B refrigerated centrifuge. The supernatant was recentrifuged at 17 500*g* for 20 min, and the pellet was resuspended in 12 mL of 0.32 M sucrose. Five milliliters of the suspension was layered on 8 mL each of 1.2 and 0.8 M sucrose, and centrifuged at 48 000*g* for 2 h. The intergradient layer containing synaptosomes was removed by gentle suction and pelleted out by recentrifugation at 27 000*g* for 20 min. The pellet was resuspended in 15 mL of 0.32 M sucrose buffered with 2 mM Tris at pH 7.4 and used immediately. The presence of synaptosomes (with seldom mitochondrial contaminants) was confirmed by electron microscopy. The concentration of synaptosomes is expressed in milligrams of protein per milliliter of

† From the Department of Physiological Chemistry, The Johns Hopkins University School of Medicine, Baltimore, Maryland 21205. *Received November 3, 1976.* This work was supported by National Institutes of Health Grant HL 18048 and National Science Foundation Grant BMS 75-08690.

[1] Abbreviations used are: ANS, 8-anilino-1-naphthalenesulfonate; DML, dimyristoyl-L-α-lecithin; Tris, 2-amino-2-hydroxymethyl-1,3-propanediol; EDTA, (ethylenedinitrilo)tetraacetic acid.

TABLE I: Relative Intensities of ANS Fluorescence in Synaptosome Suspensions in the Presence of Anesthetics.[a-c]

| Anesthetics | Concn[d] (mM) | Synaptosome | Pronase-treated synaptosome |
|---|---|---|---|
| Local anesthetics | | | |
| Lidocaine | 3.7 | 2.4 | 1.2 |
| Bupivacaine | 1.4 | 2.0 | 1.2 |
| Procaine | 4.0 | 2.2 | 1.3 |
| Sedative hypnotics | | | |
| Pentobarbital | 1.5 | 0.70 | 0.57 |
| γ-Butyrolactone | 2.2 | 0.97 | 0.84 |
| Chloral hydrate | 9.0 | 1.1 | 1.1 |

[a] The fluorescence intensities of ANS in synaptosome or Pronase-treated synaptosome suspensions are taken as a unit (1.0). [b] Synaptosome concentrations, 0.2 to 2 mg/ml. ANS concentration, $2 \times 10^{-4}$ M. [c] Solvent conditions: 0.32 M sucrose, 2 mM Tris buffer, pH 7.4, at 25 °C. [d] The concentrations given in column 2 corresponds to clinically effective concentrations of each anesthetic.

suspension, and was determined by the method of Lowry et al. (1951).

*Phospholipid and Other Chemicals.* DML was purchased from Calbiochem. This lipid was further purified in a silicic acid column using chloroform–methanol mixtures. The fraction eluted with the chloroform–methanol ratio of 30:70 (v/v) was used. Silica gel thin-layer chromatography of the purified lipid showed a single spot, indicating that free fatty acid and phosphatidic acid contamination in the commercial lipid was eliminated.

An appropriate amount of phospholipid was dispersed in 0.05 M phosphate buffer at pH 7.4 containing 0.1 N NaCl and 20 μM EDTA. Ultrasonic irradiation of DML dispersions was done with a Biosonik IV sonicator at a 100-W level for 5 min at 25 °C. After sonication, the dispersions were kept at the same temperature for 30 min to obtain maximum aggregation before suitable amounts of anesthetics were added. The mixtures were then incubated for another hour at 25 °C before use. These DML dispersions are liposomic, yet stable for reproducible results. The average diameter of the vesicles was 1000 Å, as checked by electron microscopy. Vesicles of limiting size (Huang, 1969) were prepared as described elsewhere (Tsong, and Kanehisa, 1977) but were found not suitable for the experiment because of the slow aggregation of vesicles in the phase transition region. In experiments involving synaptosome suspensions, ANS was dissolved in the NaCl–EDTA–phosphate buffer. The concentration of ANS in the final mixtures was 5 μM, less than $1/500$ the concentration of DML. No changes in the size distribution and the phase transition of DML vesicles were detected by the addition of this low level of ANS.

*Equilibrium and Kinetic Measurements.* Lipid phase transitions monitored by turbidity changes were taken with a McPherson Model 707K spectrophotometer. Equilibrium fluorescence measurements were performed in an Aminco-Bowman spectrofluorometer. The kinetic experiment was performed with a Durrum D-110 stopped-flow spectrophotometer equipped with a fluorescence kinetic attachment. Detailed experimental procedures are given elsewhere (Tsong, 1975a).

## Results

*ANS Binding to Synaptosomes.* The binding of ANS to lecithin bilayers greatly enhances its fluorescence intensity (Träuble, 1972; Jacobson and Papahadjopoulos, 1976; Tsong, 1975a). When ANS is added to synaptosome suspensions incubated with a clinically effective concentration of local anesthetics there is a further increase in fluorescence intensity (about 2.5-fold, see Table I). This enhancement was consistently observed for the three local anesthetics tested. Incubation of synaptosomes with sedative hypnotics yielded opposite results: either no significant effects with γ-butyrolactone and chloral hydrate, or suppression of the ANS fluorescence with pentobarbital (Table I). To demonstrate that this fluorescence enhancement involves alterations of the surface properties, synaptosomal suspensions were treated with Pronase to remove surface proteins. This treatment reduced by 75% the tryptophan fluorescence of synaptosomal proteins. The same ANS binding experiment was repeated for Pronase-treated synaptosomes.

The enhancement of ANS fluorescence by local anesthetics has now been reduced to only 1.2-fold (see Table I). The 1.2-fold increase in ANS fluorescence was also observed when a sonicated dipalmitoyl-L-α-lecithin dispersion was substituted for synaptosomes. Contrary to these observations, the decrease in ANS fluorescence due to pentobarbital was not greatly affected by the Pronase treatment. Table I summarizes these results.

Thus, two modes of action of local anesthetics can be conceived. First, they altered the surface properties of synaptosomes. Second, the anesthetics interacted directly with membrane lipids. The first mode of action involves changes in the state of surface proteins, although it does not necessarily mean these proteins are specific for nervous excitation. The second effect is less pronounced in the equilibrium experiment (only 1.2-fold enhancement in ANS fluorescence), but is associated with a much larger change in the rate of the probe binding to lipid bilayers, as will be shown in the following sections.

*Kinetics of ANS Permeation.* The difference between local anesthetics and sedative hypnotics as demonstrated by the enhancement of ANS fluorescence in synaptosomal membranes is small, and its significance may be in doubt. However, the effect is vividly amplified when the rate of ANS binding is measured.

When ANS is mixed with phospholipid vesicles the reaction proceeds in at least three steps (Haynes, 1972; Tsong, 1975a). The first step occurs in the submillisecond time range and involves the adsorption of ANS to the outer layer of vesicles. This reaction depends on both ANS and phospholipid concentrations (Haynes, 1972). After dye adsorption there is a rapid reorientation of the dye that takes place in the time range of 10 ms. This reaction does not increase the dye uptake (Tsong, 1975a). Under certain conditions (e.g., the temperature of the suspension near the $T_m$ of lipid phase transition) ANS can permeate into the inner layer(s) of the vesicles. As a result, the apparent concentration of bound dye increases by nearly a factor of 2 (Tsong, 1975a). This last step occurs in the second time range and has been shown to be due to a dye transport reaction (Tsong, 1975a; Haynes and Simkowitz, 1977). The ANS transport reaction (see Figure 3 of Tsong, 1975a) is extremely sensitive to the physical state of lipid bilayers.

When the rate, or the reciprocal of half-time, of ANS permeation in DML bilayers is plotted against the concentration of procaine and lidocaine, as shown in curves A and B of Figure 1, there is a dramatic enhancement near 1.3 mg/mL (4.8 mM) of anesthetics. The clinically effective concentrations of procaine and lidocaine fall in the same range. The sedative hypnotics pentobarbital and chloral hydrate, on the other hand, showed a much smaller effect (curves C and D of Figure 1).

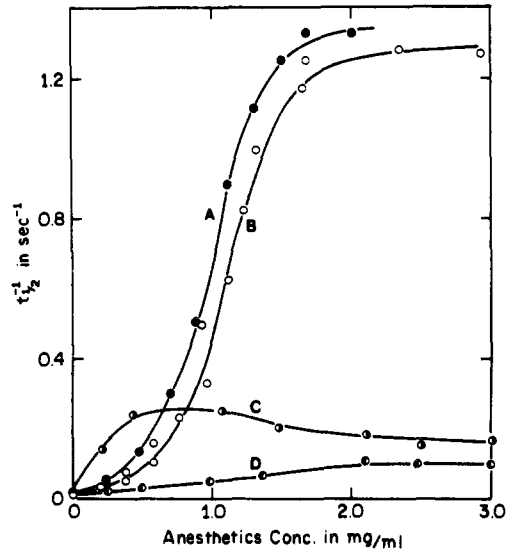


FIGURE 1: Different effects of local anesthetics and sedative hypnotics on the rate of ANS transport in DML bilayers. The rate, or the reciprocal of the half-time, of ANS transport in DML bilayers is plotted against anesthetic concentration present in the suspensions. Conditions: 0.1 N NaCl, 20 $\mu$M EDTA, in 0.05 M phosphate buffer at pH 7.4 and 22.0 °C. DML concentration, 2 mg/mL; ANS concentration, 5 $\mu$M. Curves A, B, C, and D are, respectively, for lidocaine, procaine, pentobarbital, and chloral hydrate.

Note that pentobarbital, which gave a greater rate enhancement as compared to chloral hydrate, also possesses some local anesthetic effect.

Similar experiments were performed with synaptosome suspensions with lidocaine and pentobarbital, and the result is given in Figure 2. As expected, pentobarbital does not increase the rate of ANS transport (curve C). In contrast, procaine increases the rate by 40-fold within the concentration range studied (curve A). Curve B represents Pronase-treated synaptosomes in the presence of procaine, indicating that the change in the rate is largely derived from anesthetic action on the lipid constituents of the synaptosomes.

*Effect of pH.* A question arises whether the promotion of dye transport by local anesthetics is purely the effect of charges. The three local anesthetics chosen here, namely procaine, lidocaine, and bupivacaine, are tertiary amines with p$K$ values around pH 7.4. It is conceivable that the protonated forms of these anesthetics can impose an electrostatic effect that facilitates the permeation of negatively charged ANS molecules in the lipid bilayers. This was found not to be the case.

In Figure 3 the rate of ANS transport in a DML–procaine mixture is plotted against the pH of the suspension (curve A). Although the protonated form can enhance the rate of ANS transport 50-fold, the neutral form is even more effective, approaching 250-fold. Curve B is a control with pure DML dispersions. These results clearly indicate that charge interaction can not be the dominant factor in the action of local anesthetics on the lipid bilayers. Although our experiment showed that $T_m$ of DML–procaine mixtures did not change in the pH range in Figure 3, we have not ruled out the possibility that more procaine may partition into the membrane in the neutral form.

*Effect of Phase Transition.* Many authors have suggested that anesthetics mixed with phospholipids increase the fluidity of the bilayers both in pure and in binary mixtures of lipid dispersions (Trudell et al., 1975; Lee et al., 1974; Jaine et al., 1975; Miller and Pang, 1976). Anesthetics can either promote

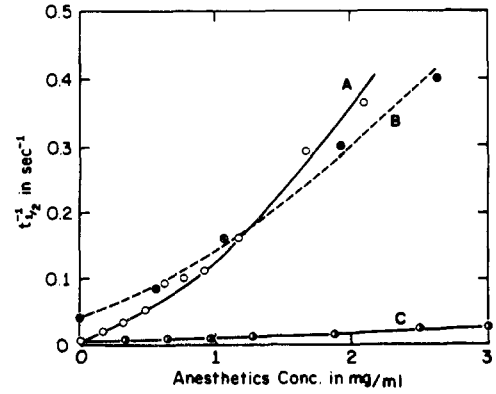


FIGURE 2: Effects of anesthetics on the ANS permeation in synaptosome membranes. The same experiment presented in Figure 1 was performed with synaptosome and Pronase-treated synaptosome suspensions. Conditions: 0.32 M sucrose in 2 mM Tris buffer at pH 7.4 and 25.0 °C. Curves A, B, and C are, respectively, data from mixtures of intact synaptosomes and lidocaine, mixtures of Pronase-treated synaptosomes and lidocaine, and mixtures of intact synaptosomes and pentobarbital. Synaptosome concentration was 1 mg of protein/mL. The concentration of Pronase-treated synaptosomes was 1 mg of protein/mL before treatment.

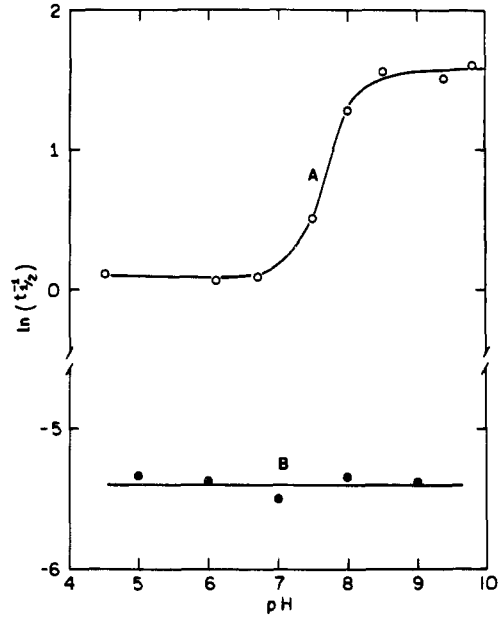


FIGURE 3: pH dependence of the rate of ANS transport in the bilayers of DML–procaine mixtures. The compositions of the final stopped-flow mixtures were 2 mg/mL of DML, 5 $\mu$M ANS in 0.1 N NaCl, 20 $\mu$M EDTA, 0.05 M phosphate at 21.5 °C. Curve A presents data from solutions containing 2 mg/mL of procaine. Curve B is a controlled experiment done with a pure DML dispersion. These results indicate that it is not the protonated form of procaine that promotes the permeation of ANS in the lipid bilayers.

the liquid-crystalline state of the single component system or induce phase separation in the binary mixtures of phospholipids. We have examined the thermotropic transition of DML dispersions in the presence of procaine by monitoring the turbidity changes (Tsong, 1974).

Figure 4 gives some selected equilibrium transition curves for a pure DML dispersion (curve A) and DML–procaine mixtures (curves B, C and D). Only the upper phase transitions (Hinz and Sturtevant, 1972; Tsong, 1974) are studied. More complete data of the equilibrium measurements are summarized in Figure 5.

Several changes by procaine on the crystalline–liquid-crystalline phase transition of DML bilayers can be seen. First,

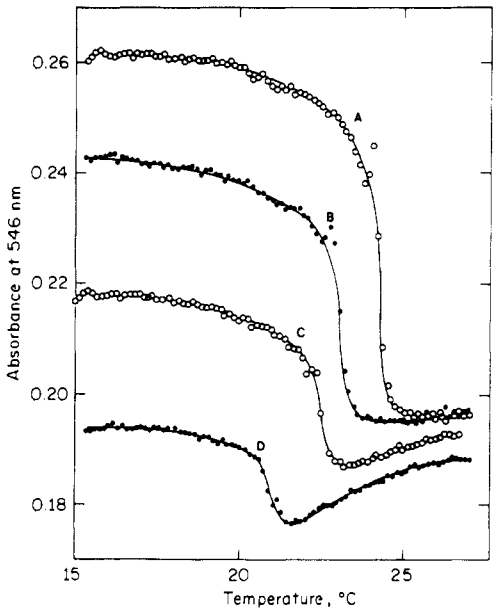


FIGURE 4: Equilibrium measurement of the crystalline-liquid-crystalline phase transition of DML-procaine mixtures. Turbidity changes of the dispersions at 546 nm are monitored in the temperature range where the upper thermotropic transition of DML bilayers occurs. Increased concentration of procaine in the lipid dispersions causes gradual diminishing of the phase transition at the same time there is a continuing broadening of the transition curves. The changes in the shape of the transition curves are further presented in Figure 5. Conditions: 2 mg/mL of DML in 0.1 N NaCl, 20 $\mu$M EDTA, in 0.05 M phosphate buffer at pH 7.4. Procaine concentrations were, respectively, 0, 0.52, 1.07, and 2.14 mg/mL for curves A, B, C, and D.

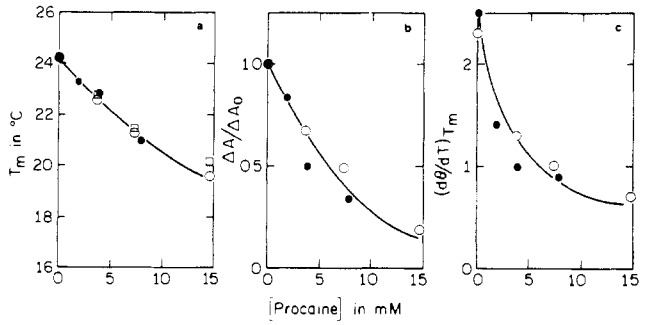


FIGURE 5: Phase transition of DML bilayers in the presence of the local anesthetic procaine. The three parameters characterizing the shape of the phase transition curves are plotted against the concentration of procaine. They are the midpoint of the transition curve, $T_m$; the total absorbance change in the transition process, $\Delta A$; and the slope of the transition curve at $T_m$, $(d\theta/dT)_{T_m}$. Experimental conditions are the same as in Figure 4. Open circles are data from dispersions with 3 mM DML, and closed circles are data from dispersions with 1.5 mM DML. The open squares are data from Figure 6. The graphical method described in Tsong et al. (1970) is adopted.

the midpoint of the transition ($T_m$) decreases, in a roughly linear fashion, as the procaine concentration is increased (Figure 5a). Second, the amplitude of the optical change due to the transition also decreases (Figure 5b). Finally, the slope at the $T_m$ of the transition decreases as the procaine concentration increases. This means that the cooperativity decreases with procaine concentration. Figure 5c plots $(d\theta/dT)_{T_m}$, in which $\theta$ is an order parameter of the bilayers, against procaine concentration. $(d\theta/dT)_{T_m}$ represents the cooperativity of the transition.

Kinetics of ANS transport are also measured in the phase-transition region of DML dispersions in the presence of various

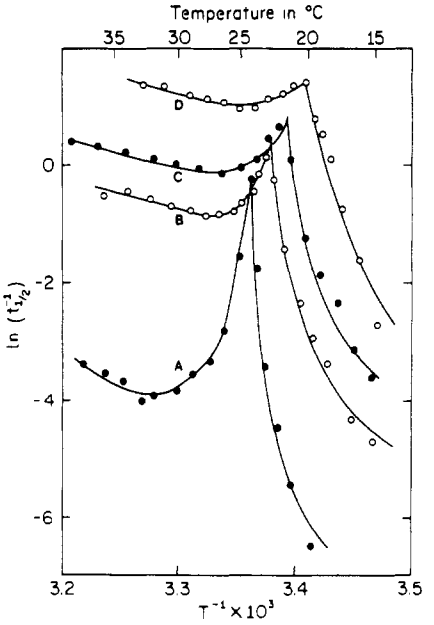


FIGURE 6: Temperature dependence of the rate of ANS permeation in the bilayers of DML-procaine mixtures. Kinetics of ANS transport is measured in the phase-transition region of DML dispersions in the presence of various concentrations of procaine. The final concentrations of DML was 2 mg/mL, and the concentrations of procaine were 0, 1, 2, and 4 mg/mL for curves A, B, C, and D, respectively. The dramatic appearance of the shape of these plots is discussed in the text.

concentrations of procaine, and the result is shown in Figure 6. This figure corresponds to the Arrhenius plot, and the slope is equivalent to the activation energy of the reaction. Curve A gives the rate of ANS permeation in a pure DML dispersion. The sharp peak at the phase-transition temperature, $T_m$, of the lipid has been reported (Tsong, 1975a,b). Simultaneous occurrences of the effects of temperature and phase transition lend the curve asymmetric. The sharpness of the peak reflects the high cooperativity of the lipid-phase transition.

When the concentration of procaine increases, the overall rate of ANS transport also increases. The dependence of rate on the phase transition also becomes less apparent. These observations are in complete accord with the result of the equilibrium study that procaine reduces both the $T_m$ and the cooperativity of the phase transition. As will be shown under Discussion, the data can be reproduced semiquantitatively by a cluster model of lipid-phase transition. According to this model, the effect of procaine is to reduce the average size of lipid clusters in the phase transition.

## Discussion

*A Cluster Model of Lipid-Phase Transition.* Three types of experimental data provide the basis for our formulation of a phenomenological description of the lipid-phase transition. They are the equilibrium transition data (Hinz and Sturtevant, 1972; Mabrey and Sturtevant, 1976; Tsong, 1974), the relaxation time of the transition process (Tsong, 1974; Tsong and Kanehisa, 1977), and the specific rate dependence of dye transport in the phase-transition region (Tsong, 1975a,b; Marsh et al., 1976).

We treat the lipid bilayer as an idealized two-dimensional Ising lattice. No detailed consideration of the chain configuration of the lipid molecule is included in this model. Instead, lipid exists in either the solid-like state (S state) or in the fluid-like state (F state). As the system approaches the transition temperature, $T_m$, from the S state, certain molecular

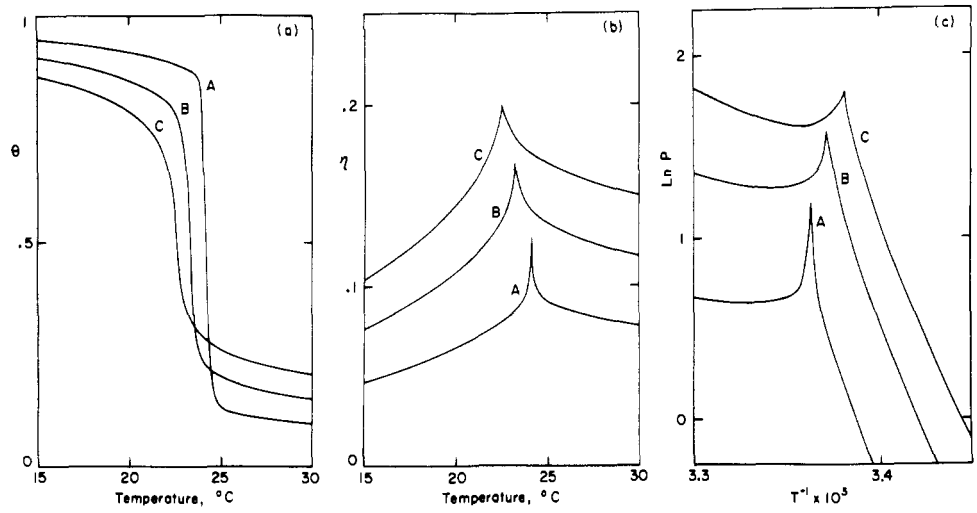


FIGURE 7: The order parameter $\theta$ of the lipid system (a), the total perimeter $\eta$ (b), and the permeability $P$ of dye molecules (c) simulated by the cluster model of lipid phase transition. The three parameters, $\theta$, $\eta$, and $P$ are defined in eq 4, 5, and 6, respectively. They are determined as follows. The finite size effect is arbitrarily chosen $l_{max} = 300$ and the enthalpy change $\epsilon$ is assumed to be 5 kcal/mol for pure DML, and 4 and 3 kcal/mol for curves B, and C, respectively. The sharpness of the transition curve (Figure 5c) is then used to determine the value of $\gamma$, which is 3.2, 3.0, and 2.9 kcal/mol for these three curves, respectively. The dye permeation is assumed to occur only at the boundary (i.e., $P_s = P_f = 0$) of clusters of size 3 or larger; that is, the summation of eq 5 is performed from $l = 3$ for c. The activation energy is $E_a = 20$ kcal/mol. The permeability is given in arbitary unit.

clusters begin to appear and grow in the otherwise uniform set of lattices. These clusters are formed with collections of molecules in the F state linked together by nearest neighbors. The free-energy state, $f(l, s)$, of a cluster with area $l$ (also the number of molecules in the cluster when each molecule is assumed to occupy a unit area) and perimeter $s$ can be expressed as

$$f(l, s) = l(\epsilon - \alpha T) + s\gamma \tag{1}$$

The first term, the bulky term, represents the free energy of elevation of $l$ molecule from the low-free-energy S state to a high-free-energy F state. The second term, the surface term, is attributed to the energy of creating phase boundaries during the transition process. Because of this boundary energy, molecules of the same state tend to aggregate in cluster form. Thus, the surface term provides the necessary cooperativity for the phase transition of lipid bilayers.

The partition function of a cluster of size $l$ is given (Fisher, 1967) by

$$q_l = g(\bar{s}) \exp\{-f(l, \bar{s})/kT\} \tag{2}$$

where $\bar{s}(l) \propto l^{\sigma}$ is the most probable or mean perimeter length of a $l$-size cluster. The combinatorial factor $g(\bar{s})$ is assumed to take the form $\lambda^{\bar{s}}/\bar{s}^{\tau/\sigma}$, by counting the number of polygons for the specific lattice structure. The numerical value of $\lambda$ is estimated to be 4.152 for the triangular lattice (Hiley and Sykes, 1961). The two phenomenological exponents $\sigma$ and $\tau$ are obtained from the exact solution for the planar Ising model to be $\sigma = 8/15$ and $\tau = 31/15$ (Fisher, 1967). If one further assumption is made that the interactions between clusters in the form of excluded volumes are neglected, then the grand partition function of the system $Q$ can be written as

$$\ln Q = \sum_{l=1}^{\infty} q_l \tag{3}$$

and the phase-transition properties can be computed.

Detailed analysis of the model and development of the computation procedures are given elsewhere (Minoru I. Kanehisa and Tian Yow Tsong, manuscript in preparation.) In this communication, we will use this model only as ground work for our elucidation of the action of local anesthetics on lipid bilayers. First, we define two thermodynamic parameters of special concern, the order parameter

$$\theta = \begin{cases} 1 - \sum_{l=1}^{\infty} l n_l & \text{below } T_m \\ \sum_{l=1}^{\infty} l n_l & \text{above } T_m \end{cases} \tag{4}$$

and the boundaries between S and F states

$$\eta = \sum_{l=1}^{\infty} s(l) n_l \tag{5}$$

Here $n_l$ is the cluster distribution function. $n_l = cq_l$, where $c$ is the normalization factor.

*Simulation of the ANS Transport Result in DML–Procaine Mixtures.* Molecular permeation in lipid bilayers depends both on the nature of the permeant and the physical state of the bilayers. If the permeant molecules are hydrophobic and miscible with phospholipids, they diffuse easily into the hydrophobic domain of these bilayers regardless of the physical state of the phospholipid. In contrast, permeation of hydrophilic molecules or ions requires a greater activation energy to overcome the bilayer barriers; hence, its rate depends strongly on the lattice arrangement of phospholipid molecules. For permeants of amphiphilic nature, the kinetics may lie between the two extremes (Tsong, 1975a). In our treatment of the kinetic data, however, we do not attempt to classify permeants by their hydrophobicity, since no generally accepted criteria are available for such a classification. Instead, we will again take a phenomenological approach.

The permeability of molecules in the lipid bilayer, $P$, is assigned the general form of

$$P \propto P_s\theta e^{-E_s/RT} + P_f(1 - \theta)e^{-E_f/RT} + P_b\eta e^{-E_b/RT} \tag{6}$$

where $P_s$, $P_f$, and $P_b$ represent, respectively, the permeability of the molecule in the S state, the F state, and the phase boundary. The exponential terms in eq 6 express the temperature dependence of the permeability, or the Arrhenius terms. For certain classes of molecules where the permeability shows a maximum at the phase-transition temperature (Papahadjopoulos et al., 1973; Blok et al., 1975; Tsong, 1975a; Marsh

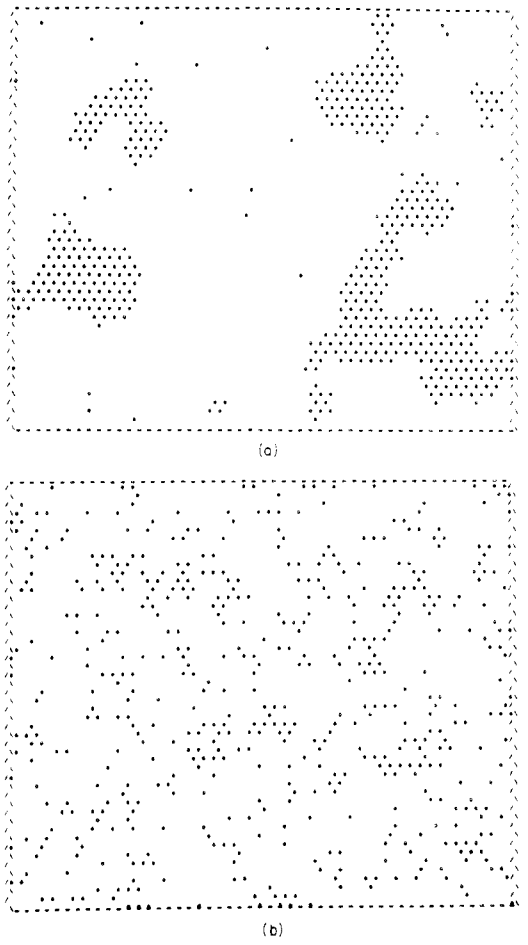


FIGURE 8: Configuration of a 50 × 50 square Ising lattice simulated for the cluster model of lipid phase transitions. The equilibrium configurations are obtained for (a) high and (b) low values of the cooperative energy $J$ between the nearest-neighbor units, using the Monte Carlo technique with periodic boundary conditions. A cluster is defined as a group of disordered units, which are denoted by asterisks, linked together by nearest-neighbor bonds. The order parameter $\theta$ is 0.79 for both cases. The cooperative energy $J$ is similar in nature to the surface tension of clusters $\gamma$ (Minoru I. Kanehisa and Tian Yow Tsong, manuscript in preparation). The numerical values of parameters used are: $\epsilon$ = 1 kcal/mol, $T_m$ = 50 °C, and $J$ = 0.6 kcal/mol for a, and $J$ = 0.1 kcal/mol for b.

et al., 1976), $p_b\eta$ dominates the kinetics of transport, since in the cluster model of the lipid phase transition there is a maximum $\eta$ at $T_m$ (see Figure 7b).

In performing the simulation one has to reproduce the equilibrium melting curves of Figure 4. The model contains four unknown parameters, $\epsilon$, $\alpha$ (or $T_m = \epsilon/\alpha$), $\gamma$, and the finite size effect $l_{max}$ at which the summation in eq 3 to 5 is truncated. The enthalpy change $\epsilon$ was estimated from the calorimetric measurements (Hinz and Sturtevant, 1972; Mabrey and Sturtevant, 1976), and we use the value of 5 kcal/mol for pure lipid. The surface tension $\gamma$ and the finite size effect $l_{max}$ affect the sharpness of the transition curve, but there is no way to separate these two effects. We use $l_{max}$ = 300 and determine $\gamma$ from Figure 5. The next step, we perform curve fittings of the data in Figure 6 by assigning suitable values for $P_s$, $P_f$, and $P_b$.

The result is given in Figure 7a, where curves A, B, and C simulate, respectively, the experimental curves A, B, and C of Figure 4. By assuming $P_s = P_f = 0$, and by using the total boundary length obtained in Figure 7b for $l \geq 3$, ANS transport can be reproduced in Figure 7c. In the figure, curves A, B, and C correspond, respectively, to curves A, B, and C of Figure 6. We have assigned the activation energy $E_b$ = 20 kcal/mol. Note, however, that, although Figure 7 reproduces the general features of the ANS transport in DML–procaine mixtures, the numerical choice for the four parameters is by no means unique.

These calculations indicate that the effect of local anesthetics on DML bilayers is to reduce the cooperativity of the lipid phase transition. In terms of the cluster model, local anesthetics reduce the average size of cluster formation in the entire temperature range. As a further illustration, the Monte Carlo technique (Metropolis et al., 1953; Binder, 1974) is used to generate cluster distributions in both highly cooperative (a) and less cooperative (b) systems, in Figure 8. Because of this shift to small size clusters in the less cooperative system, the total phase boundaries of the lattices increase, permitting faster permeation of ANS in lipid bilayers.

## Summary

Anesthetics interact with both membrane proteins and lipids. Only the latter is examined in some detail. It is shown that the mode of action of local anesthetics and sedative hypnotics is distinctively different in their ability to alter ANS permeability in lipid bilayers of synaptosomes and DML dispersions. In the case of local anesthetics, the clinically effective concentration correlates well with the concentration for maximum enhancement in the rate of ANS transport. These observations indicate that at this concentration there is a critical change in lipid bilayer structure. A cluster model of lipid phase transitions suggests that this change may correspond to a shift in the average size of lipid clusters in bilayers. In biological membranes this could mean a homogenization of different lipid components into a more fluid-like phase.

## References

Binder, K. (1974), *Adv. Phys. 23,* 917.
Blaustein, M. P. (1968), *J. Gen. Physiol. 51,* 293.
Blaustein, M. P., and Goldman, D. E. (1966), *J. Gen. Physiol. 49,* 1043.
Blok, M. C., Van der Neut-Kok, E. C. M., Van Deenen, L. L. M., and De Gier, J. (1975), *Biochim. Biophys. Acta 406,* 187.
Condouris, G. A. (1963), *J. Pharmacol. Exp. Therap. 141,* 253.
Denburg, J. L., Eldefrawi, M. E., and O'Brien, R. (1972), *Proc. Natl. Acad. Sci. U.S.A. 69,* 177.
Eyring, H. (1966), *Science 154,* 3757.
Fisher, M. E. (1967), *Physics 3,* 255.
Haynes, D. H. (1972), *DECHEMA—Monogr. 71,* 119.
Haynes, D. H., and Simkowitz, P. (1977), *J. Membr. Biol.,* manuscript submitted for publication.
Hiley, B. J., and Sykes, M. F. (1961), *J. Chem. Phys. 34,* 1531.
Hinz, H.-J., and Sturtevant, J. M. (1972), *J. Biol. Chem. 247,* 6071.
Hoss, W., and Abood, L. G. (1974), *Eur. J. Biochem. 50,* 177.
Huang, C. (1969), *Biochemistry 8,* 344.
Jacobson, K., and Papahadjopoulos, D. (1976), *Biophys. J. 16,* 549.
Jain, M. K., Wu, N. Y., and Wray, L. W. (1975), *Nature (London) 255,* 495.
Lee, A. C. (1976), *Nature (London) 262,* 545.
Lee, A. G., Birdsall, N. J. M., Metcalfe, J. C., Toon, P. A., and Warren, G. B. (1974), *Biochemistry 13,* 3699.
Lowry, O. H., Rosebrough, N. J., Farr, A. L., and Randall, R.

J. (1951), *J. Biol. Chem. 193,* 265.
Marbrey, S., and Sturtevant, J. M. (1976), *Proc. Natl. Acad. Sci. U.S.A. 73,* 3862.
Marsh, D., Watts, A., and Knowles, P. F. (1976), *Biochemistry 16,* 3570.
Metropolis, N., Rosenbluth, A. N., Rosenbluth, M. N., and Teller, A. H. (1953), *J. Chem. Phys. 21,* 1087.
Miller, K. W., and Pang, K. Y. (1976), *Nature (London) 263,* 253.
Miller, K. W., Paton, W. D. M., Smith, R. A., and Smith, E. B. (1973), *Mol. Pharmacol. 9,* 131.
Naharashi, T., Moore, J. W., and Poston, R. N. (1969), *J. Neurobiol. 1,* 3.
Papahadjopoulos, D. (1972), *Biochim. Biophys. Acta 265,* 169.
Papahadjopoulos, D., Jacobson, D., Nir, S., and Isac, T. (1973), *Biochim. Biophys. Acta 311,* 330.
Seeman, P. (1975), in Cell Membranes, Weissmann, G., and Claiborne, R., Ed., New York, N.Y., HP Publishing Co., pp 239–247.
Seeman, P., and Roth, S. (1972), *Biochim. Biophys. Acta 255,* 171.
Thesleff, S. (1956), *Acta Physiol. Scand. 37,* 335.
Träuble, H. (1972), *Biomembranes 3,* 197.
Trudell, J. R., Payan, D. G., Chin, J. H., and Cohen, E. N. (1975), *Proc. Natl. Acad. Sci. U.S.A. 72,* 210.
Tsong, T. Y. (1974), *Proc. Natl. Acad. Sci. U.S.A. 71,* 2684.
Tsong, T. Y. (1975a), *Biochemistry 14,* 5409.
Tsong, T. Y. (1975b), *Biochemistry 14,* 5415.
Tsong, T. Y., and Kanehisa, M. I. (1977), *Biochemistry 16* (in press).
Tsong, T. Y., Hearn, R. P., Wrathall, D. P., and Sturtevant, J. M. (1970), *Biochemistry 9,* 2666.
Weber, M., and Changeux, J. P. (1974), *Mol. Pharmacol. 10,* 35.

# Biosynthesis of the Polyoxins, Nucleoside Peptide Antibiotics: Biosynthetic Pathway for 5-*O*-Carbamoyl-2-amino-2-deoxy-L-xylonic Acid (Carbamoylpolyoxamic Acid)†

Shunji Funayama and Kiyoshi Isono*

ABSTRACT: The biosynthetic pathway for 5-*O*-carbamoyl-2-amino-2-deoxy-L-xylonic acid (carbamoylpolyoxamic acid) was studied. This unusual amino acid is an N terminus of the nucleoside peptide antibiotics, the polyoxins, produced by *Streptomyces cacaoi* var. *asoensis*. The pathway, glutamate → glutamate-γ-semialdehyde → α-amino-δ-hydroxyvalerate → α-amino-δ-carbamoyloxyvalerate → 5-*O*-carbamoyl-2-amino-2-deoxy-L-xylonate → polyoxins, was established by the following experimental evidence: (1) Two intermediate amino acids, DL-[5-$^{14}$C;2-$^{3}$H]-α-amino-δ-hydroxyvaleric acid and DL-[*carbamoyl*-$^{14}$C]-α-amino-δ-carbamoyloxyvaleric acid, were synthesized and fed to growing cells of *S. cacaoi*. Both amino acids were incorporated into carbamoylpolyoxamic acid with high efficiency without randomization. However, tritium was lost almost completely. (2) DL-[5-$^{14}$C;2-$^{3}$H; *amino*-$^{15}$N]-α-Amino-δ-hydroxyvaleric acid was synthesized and fed to washed cells. Dilution factors for $^{14}$C, $^{3}$H, and $^{15}$N were 10, 52, and 22, respectively. This result can be reasonably explained by functioning of transaminase(s), and the incorporation of the intact α-amino acid structure of α-amino-δ-hydroxyvaleric acid into that of carbamoylpolyoxamic acid is indicated. (3) In vivo experiments showed that [$^{14}$C]carbonate was incorporated into C-1 and the carbamoyl carbon of carbamoylpolyoxamic acid. Further, a cell-free extract of *S. cacaoi* was able to synthesize [*carbamoyl*-$^{14}$C]-α-amino-δ-carbamoyloxyvaleric acid from α-amino-δ-hydroxyvaleric acid and [$^{14}$C]carbamoyl phosphate. Partially purified ornithine carbamoyltransferase of this organism was shown not to be able to use α-amino-δ-hydroxyvalerate as a substrate. (4) Biosynthetically prepared [1, *carbamoyl*-$^{14}$C]carbamoylpolyoxamic acid was incorporated intact into the polyoxins with the incorporation ratio of 48%, whereas [$^{14}$C]polyoxamic acid was not appreciably incorporated.

The nucleoside peptide antibiotics, the polyoxins, are the metabolites of *Streptomyces cacaoi* var. *asoensis* (Isono et al., 1969). The general structure is shown in Scheme I. In our biosynthetic study of this group of antibiotics, we have shown that the 5-substituted uracil base of the polyoxins is biosynthesized from uracil and C-3 of serine (Isono and Suhadolnik, 1976; Funayama and Isono, 1976). 5-Fluorouracil can replace uracil to form the aberrant 5-fluoropolyoxins (Isono et al., 1973; Isono and Suhadolnik, 1976). It was also shown that the intact carbon skeleton of L-isoleucine is incorporated into 3-ethylidene-L-azetidine-2-carboxylic acid, a C-terminal amino acid of the polyoxins (Isono et al., 1975).

5-*O*-Carbamoyl-2-amino-2-deoxy-L-xylonic acid (carbamoylpolyoxamic acid, CPOAA[1]) is an N-terminal amino acid common to all the biologically active polyoxins. In our

† From the Institute of Physical and Chemical Research, Wako-shi, Saitama 351, Japan. *Received January 17, 1977.* This work was supported in part by a grant for the studies on "Life Science" at the Institute of Physical and Chemical Research.

[1] Abbreviations used are: POAA, 2-amino-2-deoxy-L-xylonic acid (polyoxamic acid); CPOAA, 5-*O*-carbamoyl-2-amino-2-deoxy-L-xylonic acid (carbamoylpolyoxamic acid); AHV, α-amino-δ-hydroxyvaleric acid; ACV, α-amino-δ-carbamoyloxyvaleric acid; DEAE, diethylaminoethyl.